SYNTHESIS, CHARACTERIZATION, AND PROCESSING OF MONOSIZED CERAMIC POWDERS

Bruce Fegley, Jr.* and Eric A. Barringer*,**
*Ceramics Processing Research Laboratory and Materials Processing Center,
** Dept. of Materials Science and Engineering, MIT, Cambridge, MA 02139

ABSTRACT

Controlled alkoxide hydrolysis reactions for the synthesis of monodispersed oxide powders are described. The chemical and physical properties of representative monodispersed powders of TiO_2, doped TiO_2, ZrO_2, doped ZrO_2, SiO_2, doped SiO_2, and ZrO_2-Al_2O_3 are described. The importance of surface chemistry for control of powder dispersion and packing is discussed and related to the control of sintered microstructures.

CONTROLLED CHEMICAL SYNTHESIS OF OXIDE POWDERS

Thermal decomposition and hydrolysis of metal alkoxides have been used to prepare a variety of high-purity oxide powders [1]. However, the major objective of this work was not to control the size distribution and shape of the resulting powders, which were generally very fine (< 100Å) and highly agglomerated. Thus, the subsequent processing of the powders to uniform fine-grained, low porosity ceramic bodies was generally not achieved and the full advantages of the alkoxide synthesis techniques for microstructure control were not realized.

Controlled hydrolysis reactions of metal alkoxides have been utilized to prepare monodispersed oxide powders of controlled size, shape, and composition, e.g., TiO_2, doped TiO_2, ZrO_2, doped ZrO_2, SiO_2, doped SiO_2, and ZrO_2-Al_2O_3. The synthetic methods used to prepare these materials involve fairly simple solution chemistry, but give a high degree of control and reproducibility. Basically, a dilute solution (~ 0.2 to 0.4 M) of the respective metal alkoxide in 200 proof anhydrous ethanol is hydrolyzed by adding an equal volume of a solution of deionized water in anhydrous ethanol. The second solution is poured into the first solution with stirring. The hydrolysis reactions are conducted in a glove box under a dry N_2 atmosphere and generally at room temperature (~ 25°C); precipitation of a white powder occurs in several seconds to several minutes. The precipitation time increases as the concentration of either the alkoxide solution or the water solution is decreased. The hydrolysis reaction may be schematically represented by the general equation

$$M(OR)_x + \frac{x}{2} H_2O = MO_{x/2} + xROH \qquad (1)$$

where x is a function of the valence of the metal cation.

After precipitation, the powder is washed by centrifuging and redispersing in distilled water (or other solvent); this cycle is repeated two to three times. The powder is then further processed by adding cation dopants or is sedimented into compacts for sintering studies. The synthesis and processing of the various oxide powders are briefly reviewed in the following sections.

Pure TiO_2

Barringer and Bowen [2] described the synthesis of monodispersed, spheroidal TiO_2 by the controlled hydrolysis of dilute solutions of titanium tetraethoxide, $Ti(OC_2H_5)_4$. In a typical experiment, a 0.30 M solution of

Mat. Res. Soc. Symp. Proc. Vol. 32 (1984)

$Ti(OC_2H_5)_4$ in 200 proof anhydrous ethanol was hydrolyzed by adding a 1.2 M solution of deionized water in ethanol. Precipitation of TiO_2 powder in ~83% yield occurred in ~5 seconds (at 25.5°C). The mean size of the TiO_2 particles, which was visually estimated from SEM micrographs, was 0.38μm. Figure 1a is a TEM micrograph of TiO_2 made by the hydrolysis of $Ti(OC_2H_5)_4$.

Titania was also prepared by the hydrolysis of several other titanium alkoxides: Titanium tetraisopropoxide, $Ti(^iOC_3H_7)_4$, titanium tetrabutoxide, $Ti(OC_4H_9)_4$, and titanium tetra-2-ethylhexoxide, $Ti(OC_8H_{17})_4$. The latter two reactions were conducted in ethanol, while the $Ti(^iOC_3H_7)_4$ was hydrolyzed in isopropanol and in ethanol. The hydrolysis reactions gave TiO_2 powders which were equiaxed, but were multinuclear and agglomerated. Typically, 0.30 M alkoxide solutions were hydrolyzed by adding 1.8 M water solutions with stirring. Precipitation occurred in ~20 seconds at 25°C. Equiaxed particles ranging in size from ~0.3μm to 0.7μm were produced and doublets, triplets, and more agglomerated particles were also formed. The agglomeration may be due to the failure of these alkoxide hydrolysis reactions to simultaneously satisfy the conditions required for formation of monodispersed, spheroidal particles [2]. A TEM micrograph of TiO_2 made by the hydrolysis of $Ti(^iOC_3H_7)_4$ is shown in Barringer and Bowen [2].

Pure ZrO_2

We have previously reported the preparation of monodispersed, spheroidal ZrO_2 by the controlled hydrolysis of zirconium normal- and isopropoxides [3]. Typically, $Zr(^nOC_3H_7)_4$ in ethanol (~ 0.10 M) was hydrolyzed with an excess of water (~ 0.5 M in ethanol). The hydrolysis was done at 50°C and precipitation of a white powder occurred in approximately two minutes. $Zr(^iOC_3H_7)_4$ in ethanol (~ 0.11 M) was hydrolyzed by an excess of water (~ 0.92 M in ethanol); at 25°C precipitation occurred in ~11 seconds and gave ZrO_2 in ~95% yield. Figure 1b is a TEM micrograph of ZrO_2 made by the hydrolysis of $Zr(^nOC_3H_7)_4$. ZrO_2 made from hydrolysis of Zr isopropoxide is approximately the same size (visually estimated from SEM micrographs), but is equiaxed rather than spheroidal and is more agglomerated [12].

Pure SiO_2

Monodispersed SiO_2 was prepared by a refinement of the procedure of Stober et al [4]. Tetraethylorthosilicate (TEOS) was hydrolyzed by a mixture of NH_4OH and H_2O (in ethanol); typically final solution concentrations were 0.3 M TEOS, 2.0 M NH_3, and 8.0 M H_2O. For these concentrations, turbidity was observed after approximately four minutes and powder with an average diameter of 0.55μm (standard deviation = 0.04μm) was obtained [5].

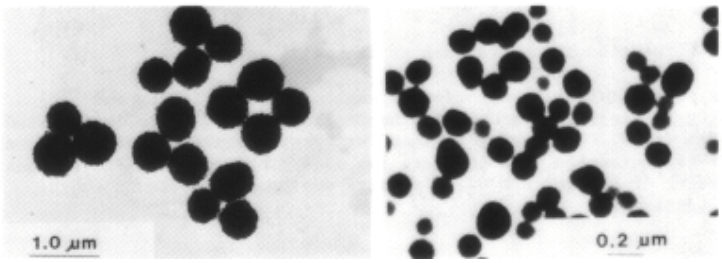

FIG. 1. (a) TEM micrograph of TiO_2 from $Ti(OC_2H_5)_4$, 0.30M; $[H_2O]$=0.90M, 25°C. (b) TEM micrograph of ZrO_2 from $Zr(^nOC_3H_7)_4$, 0.09 M; $[H_2O]$=0.5M, 50°C.

Doped TiO_2

Singly- and doubly-doped TiO_2 powders were prepared by the alkoxide hydrolysis process and by inorganic salt precipitation [6,7]. TiO_2 powders singly doped with either Ta_2O_5 or Nb_2O_5 were made by the controlled cohydrolysis of dilute solutions of $Ti(OC_2H_5)_4$ (~ 0.2 M) and either $Ta(OC_2H_5)_5$ or $Nb(OC_2H_5)_5$ (~ $5x10^{-4}$ M). Again, ethanol was used as a solvent and a water solution in ethanol was poured, with stirring, into the alkoxide solution. TiO_2 powders doubly doped with BaO, CuO, or SrO and either Ta_2O_5 or Nb_2O_5 were made by precipitating the respective metal carbonate onto the singly-doped particles, which were dispersed in a dilute aqueous solution of the respective metal chloride. The precipitation was conducted by adding an excess of $(NH_4)_2CO_3$ to the dispersion with stirring. Figure 2a is a SEM micrograph of Nb_2O_5, BaO-doped TiO_2.

The alkoxide cohydrolysis reactions involved in the synthesis of singly-doped TiO_2 are schematically represented by the general equation

$$Ti(OC_2H_5)_4 + M(OC_2H_5)_5 + H_2O = TiO_2 \cdot M_2O_5 \cdot XH_2O \qquad (2)$$

where M is Ta or Nb and X ~ 1/2. The carbonate precipitation reactions involved in the synthesis of doubly-doped TiO_2 powders are schematically represented by the general equation

$$M'Cl_2(aq) + (NH_4)_2CO_3(aq) = M'CO_3 \text{ (on particles)} \qquad (3)$$

where M' is Ba, Cu, or Sr. Doped TiO_2 powders containing SrO were also made by the cohydrolysis of $Ti(OC_2H_5)_4$ and $Sr(^iOC_3H_7)_2$.

Doped ZrO_2

Y_2O_3-doped ZrO_2 was made by the cohydrolysis of $Zr(^nOC_3H_7)_4$ and $Y(^iOC_3H_7)_3$. The solid yttrium isopropoxide was dissolved in the $Zr(^nOC_3H_7)_4$ and this solution was then dissolved in ethanol. The resulting solution was ~ 0.08 M $Zr(^nOC_3H_7)_4$ and ~ 0.01 M $Y(^iOC_3H_7)_3$, appropriate for making 6.3 mole % Y_2O_3-doped ZrO_2. Precipitation of a white powder was instantaneous at 50°C. Figure 2b is a SEM micrograph of Y_2O_3-doped ZrO_2 [13].

Doped SiO_2

Monodispersed B-doped SiO_2 particles [7,8] were made by partially hydrolyzing TEOS, adding tri-n-butyl borate (TBB), $B(OC_4H_9)_3$, and then completely hydrolyzing this mixture. A range of TEOS/H_2O concentrations and

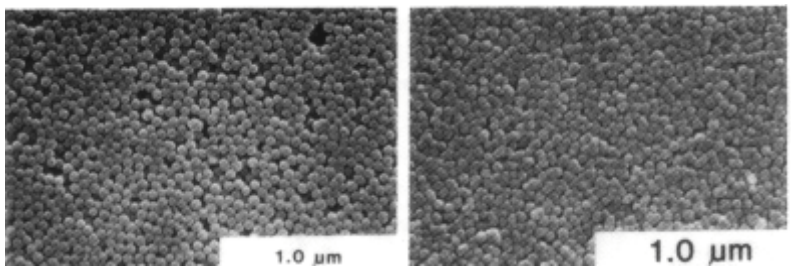

FIG. 2. (a) SEM micrograph of the top surface of a gravity sedimented compact of Nb_2O_5 (0.5 wt. %), BaO(0.2 wt. %) -doped TiO_2. (b) SEM micrograph of Y_2O_3 (6.5 mol %) -doped ZrO_2 powder.

B/Si ratios were investigated [8]. Typically, the final concentrations were 0.01-0.20 M TEOS, ~5 M H_2O, and ~2 M NH_3; the TBB/TEOS molar ratios were 0.5-2.0. Figure 3a is a TEM micrograph of B-doped SiO_2 made from 0.01 M TEOS and having a nominal B/Si ratio of 1:1 [8].

ZrO_2-Al_2O_3

Two-phase particles containing ZrO_2 and Al_2O_3 were made by the hydrolysis of $Zr(^nOC_3H_7)_4$ in an ethanolic dispersion of Al_2O_3 particles (Alcoa XA139 superground) [9]. Typically, several grams of Al_2O_3 powder, which had previously been classified to give a 0.2-0.3μm size fraction [10], was dispersed in 500 ml ethanol and mixed with a $Zr(^nOC_3H_7)_4$ solution in ethanol giving an approximately 0.03 M alkoxide solution. This was hydrolyzed with an excess of water (~ 0.3 M in ethanol) at 50°C. No observable change in the dispersion, which was already white, occurred after the hydrolysis. Figure 3b shows a TEM micrograph of ZrO_2-Al_2O_3 powder [9].

CHEMICAL AND PHYSICAL CHARACTERIZATION OF OXIDE POWDERS

Characterization of the chemical and physical properties of the oxide powders is critical for control of powder dispersion, packing and sintering. Some of the important physical properties are particle size distribution, shape, surface area, density, and crystal structure. Among the important chemical properties are bulk composition, dopant levels, dopant homogeneity, impurity content, and surface/liquid interfacial chemistry. A variety of techniques are available to measure these properties; some yield acceptable results, while others do not. The techniques utilized in our research and results for the different oxide powders, which are summarized in Table I, are briefly reviewed in the following sections. More detailed descriptions, which cannot be presented here because of space limitations, are given elsewhere in the literature [2, 6-13].

Particle Size, Size Distribution and Shape

Assessments of particle shape, state of agglomeration, and qualitative size distributions were obtained from SEM and TEM micrographs. Quantitative size distributions were obtained for >500 particles from TEM micrographs using a histogram method [11]; image analysis and direct counting were used to generate the histograms. Although this technique is precise, especially when >1000 particles are counted, it is time consuming and tedious. In addition, differentiation between hard agglomerates (aggregates) and flocs formed during sample preparation and drying was often difficult.

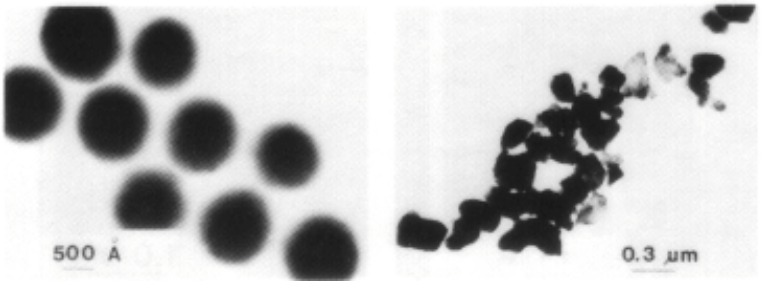

FIG. 3. (a) TEM micrograph of B-doped SiO_2 with a nominal B/Si ratio of 1:1. (b) TEM micrograph of ZrO_2-Al_2O_3 powder with a nominal ZrO_2 content of 20 volume percent.

More rapid techniques based on particle sedimentation and laser light scattering were also utilized. The Sedigraph unit (Micromeritics), based on X-ray absorption for sedimenting particles, worked well for several powders having a mean diameter >0.3μm. Dynamic laser light scattering (photon correlation spectroscopy, PCS) using the Coulter Model N4D gave rapid and accurate results for the uniform-size powders. This instrument utilized the cummulant analysis method to determine the Brownian diffusion coefficient and the hydrodynamic size.

Figures 1-3a illustrate that to a good first approximation the oxide particles produced by the controlled alkoxide hydrolysis reactions are monodispersed, spheroidal, and predominantly singlets. Table I lists representative values of the average particle size and size range (for ranges of reagent concentrations) for eight oxide powders. These data were obtained by a variety of techniques; correlation between techniques for a powder was generally excellent.

Physical Measurements (Surface Area, Density, Crystallinity)

The data on other physical properties such as surface area, density, and crystallinity are also summarized in Table I. All particles produced by the alkoxide hydrolysis technique were amorphous, as determined by X-ray and electron diffraction. The densities of the amorphous powders, measured by a stereopycnometer (Quantachrome Corp.) using He gas, were generally less than (by > 20%) the densities of the stable low-temperature modifications of the crystalline oxides. However, the silica particles were only 5% less dense than fused silica.

Specific surface areas were measured by multipoint BET (Quantachrome Corp.), using N_2 gas as the adsorbate and assuming a cross-sectional area of $16.2Å^2$. The B.E.T. surface areas were found to depend upon the initial washing of the powders. Powders washed in ethanol had lower surface areas (larger equivalent spherical diameters) than powders washed in water. Barringer [11] discussed this observation for pure TiO_2 and attributed it to a surface coating of fine spherical precipitates resulting from the rapid hydrolysis of residual (unreacted) $Ti(OC_2H_5)_4$ on the particle surface upon contact with water in the initial washing step (see Fig. 1a). TEM micrographs of ethanol-washed and water-washed ZrO_2 suggest that an analogous effect causes the higher surface areas of water-washed ZrO_2. The equivalent spherical diameters of the ethanol-washed ZrO_2 are in the range 0.12-0.22μm and span the mean particle sizes determined by TEM and PCS.

Chemical Analyses

Several methods have been used to determine dopant and impurity levels and volatile contents of the oxide powders. The results of the various analytical techniques are briefly reviewed below. More complete descriptions are given elsewhere in the literature [6-13].

Volatile contents of the powders were generally estimated by simultaneous DTA/TGA analysis. Water washed TiO_2 contained 10-16% (weight) water; carbon analysis of the as-synthesized powder showed 0.18% (weight) carbon [2]. The doped TiO_2 powders showed variable weight losses which correlated with their processing prior to DTA/TGA analysis. Powders that were not washed or not dried at 80°C lost the most weight, 21%, while powders which had been washed and then calcined at 450°C for 30 minutes lost the least weight, 2-5%. Most of the observed weight loss was due to the loss of water of hydration, which was removed below 200°C. DTA/TGA analysis of the pure ZrO_2 showed 14-20% weight loss, depending on the temperature at which the hydrolysis reaction was conducted and the subsequent processing of the powder. Carbon analyses of the water-washed ZrO_2 made by hydrolysis of Zr n-propoxide showed 1.02-1.07% carbon, presumably due to residual alkoxide.

Dopant contents and cation impurity levels in the oxide powders were mainly determined by inductively coupled plasma emission spectroscopy (ICP), and also by direct coupled plasma emission spectroscopy (DCP), instrumental neutron activation analysis (INAA), and semiquantitative emission spectroscopy. Sintered ceramics were analyzed by ICP, electron probe microanalysis (EPMA), and proton induced X-ray emission (PIXE).

The cation impurity levels in the pure TiO_2 made by hydrolyzing $Ti(OC_2H_5)_4$ were determined by semiquantitative emission spectroscopy and ICP. The former method showed <10 ppm Al, Ca, Cu, and Mg and <100 ppm Si, while the latter gave 40 ppm Ca and 80 ppm Si. EPMA wavelength dispersive analysis gave 90 ppm Si in a sintered TiO_2 ceramic. Cation impurities in pure ZrO_2 made by hydrolysis of Zr n-propoxide and isopropoxide were determined by ICP analyses of powders and EPMA analyses of sintered ceramics. ZrO_2 made from the n-propoxide contains ~ 1.3% (weight) Hf, while ZrO_2 made from the isopropoxide contains <100 ppm Hf. (PIXE analysis of a sintered ZrO_2 ceramic made from the isopropoxide gave 57 ppm Hf, ICP analysis of the powder gave <93 ppm Hf). Otherwise, the major cation impurities in the ZrO_2 are Al (<160 ppm), Fe (100-150 ppm), and Si (60-400 ppm). (Ti is present at ~ 350 ppm, but may be due to Ti contamination from the ultrasonic probe tip used to disperse the powder during processing.) The rather high and variable Si contents may be contamination from bottles used to store the alkoxides or from glassware used for the hydrolysis reactions.

The dopant levels in the doped TiO_2 powders and ceramics were determined by ICP, DCP, EPMA and INAA analyses. The Y_2O_3 level in the Y_2O_3-doped ZrO_2 ceramics was determined by EPMA and PIXE analyses. The boron level in the doped SiO_2 was determined by ICP. The results of these extensive analyses demonstrate that the controlled alkoxide hydrolysis reactions give exceptional control over the desired chemistry, with a low level of contaminants. This feature has also been emphasized by Mazdiyasni [1]. However, more importantly, this control over the chemistry is coupled with control of the particle size distribution and morphology. Results presented by Fegley et al [4] show that the doped TiO_2 powders are homogeneously doped with the Nb^{5+} or Ta^{5+} cations and that the Ba^{2+}, Cu^{2+}, Sr^{2+} cations are present on the surface of the TiO_2 particles. EPMA analyses of Y_2O_3-doped ZrO_2 ceramics show that the grain to grain homogeneity of the Y_2O_3 dopant is actually better than the homogeneity of the HfO_2 impurity.

SURFACE CHEMISTRY, POWDER DISPERSION AND PACKING

The state of aggregation of a dispersed powder and the subsequent packing into green bodies, both of which significantly affect the sinterability and final microstructure, depend on the stability of the dispersion against coagulation. Coagulation processes are controlled by the interparticle forces which are dependent on the physical characteristics and the powder/solvent interfacial chemistry. An understanding of the interfacial chemistry (particle-solvent-solute interactions) is critical to the development and control of reliable fabrication processes. For instance, the casting of an aqueous, surfactant-stabilized Al_2O_3 slip may yield dense, uniformly-packed bodies ($\rho \approx 70\% \rho_{th}$) at pH ≈ 7-8, and yet yield porous bodies at pH ≈ 3. However, for aqueous dispersions without the surfactant this behavior is reversed.

Dispersion and Stability

The stability of a dispersion against coagulation depends on the sign and magnitude of the particle interaction energies. The frequency of

Brownian encounters determines the maximum rate of coagulation in the absence of forces; however, coagulation is retarded by the presence of repulsive interactions. The general equation describing two-body interactions consists of attractive and repulsive terms:

$$V_T = V_A(\text{van der Waals}) + V_R(\text{electrostatic}) + V_R(\text{steric}) + V_R(\text{others}). \quad (4)$$

The van der Waals attractive forces between particles, due to electronic fluctuations of the atoms within particles, depend on the dielectric properties of the particle and solvent through the Hamaker constant [14]. This force can be modified by the presence of an adsorbed solute layer, e.g., polymer surfactant [15].

The electrostatic repulsion is caused by the interaction of electrical double layers surrounding the dispersed particles, which arises from the particle surface/solvent acid-base reactions and electrolyte redistribution around the particles. The magnitude of the repulsion depends on the solvent dielectric constant and pH (surface charging) and the indifferent electrolyte concentration (electrostatic shielding); excellent reviews exist in the literature [16,17].

The nature of steric forces, due to the interaction of macromolecules adsorbed onto particle surfaces, is not as well understood as electrostatic forces; however, it is presently the topic of extensive investigation. These forces depend on the macromolecule structure and size (MW), mode of adsorption and adsorption density, and conformation. The interplay of solvent-polymer (solvation), solvent-surface (wetting), and surface-polymer (adsorption) interactions control steric stabilization; excellent reviews are given by Tadros [18] and Sato and Ruch [19]. The chemistries in the systems used in manufacturing must be better understood for reproducible fabrication of ceramic materials; the Al_2O_3 example previously cited is representative of such systems.

Although no precise rules can be stated regarding the formation of stable dispersions, some guidelines can be stated. In polar, protic solvent electrostatic forces may be the dominant repulsive component; in such systems stability requires a low electrolyte concentration (< 0.01 M) and a solution pH several units above or below the isoelectric point (IEP). In nonpolar and aprotic solvents steric stabilization is required. The most effective surfactants (dispersants) have strongly adsorbed functional groups and strongly solvated segments in the macromolecule. In mixed systems (polar solvents and surfactants) the interactions are complex; simple guidelines are not possible. In all cases, though, the stability of the dispersions can be assessed qualitatively by sedimentation techniques [20] or quantitatively by measuring the change in average particle size with time [21].

POWDER PACKING AND SINTERING

The goal of ceramic processes is to control particle packing in green microstructures, and thus control sintered microstructures and properties. The critical relationship between green and sintered microstructures in obtaining fine-grain, dense ceramics has been established [2,22,23]. In all cases studied (TiO_2, ZrO_2, SiO_2, B-SiO_2), stable dispersions were formed in deionized water with a pH several units above or below the IEP: TiO_2 at pH = 4, 8-10 (IEP = 5-6); ZrO_2 at pH = 4, 9-11 (IEP = 6-7.5); SiO_2 and B-SiO_2 at pH $>$ 5 (IEP = 2-3). Figures 4 (ZrO_2, pH = 10) and 5 (SiO_2, pH = 7) show representative examples of top and fracture surfaces of

compacts formed by sedimentation from stable dispersions. The packing is extremely uniform and reproducible (from sample to sample); the voids present are about one particle diameter in size (0.2-0.4 μm).

The sintering process not only depends on the particle size (scaling laws), but also on the particle packing density and uniformity. This dependence was demonstrated for pure TiO_2 by Barringer and Bowen [2,11,23,24]; identical behavior was observed for all powder systems (the details of these studies are discussed in later publications). Figure 6 shows the microstructure of a ZrO_2 compact sintered for 1.5 hours at 1160°C; a dense ($\rho > 98\% \rho_{th}$), uniform, fine-grain ($\bar{d} \approx 0.2$ μm), structure is observed. Essentially no grain growth occured and all pores are intergranular and small relative to the grain size. The sintering temperature of this compact, which had an initial density of ~65% of theoretical, was 400-500°C below that required for conventional ZrO_2 powders. Figure 7a demonstrates that B-SiO_2 can be densified at temperatures approaching 700°C [8].

Porous compacts, when sintered under conditions similar to those used for dense compacts, yielded uniformly porous bodies. Such structures have potential as filter membranes, chromatography substrates, catalytic substrates and sensor elements. As an example, Figure 7b shows a porous SrO-doped TiO_2 body (0.52 mole percent SrO) sintered for 2.5 hours at 1100°C. The grains ($\bar{d} \approx 0.4$-0.6 μm) and pores are uniform in size and spatial distribution. The discrete particles on the larger TiO_2 grains may be $SrTiO_3$ precipitates [25].

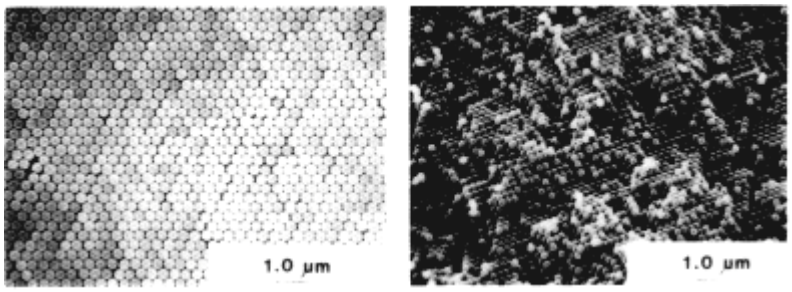

FIG. 4. (a) SEM micrograph of the top surface of a gravity sedimented compact (pH = 10) of ZrO_2. (b) Fracture surface of the same compact.

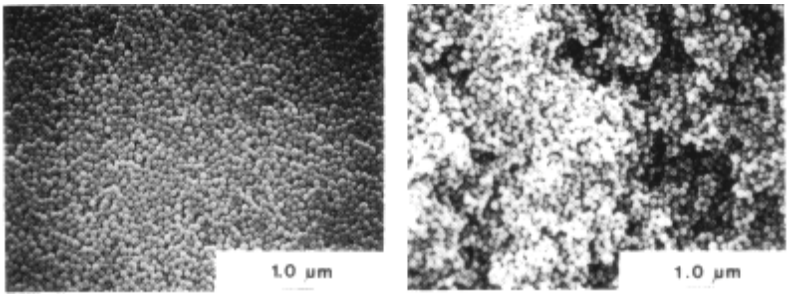

FIG. 5. (a) SEM micrograph of the top surface of a gravity sedimented (pH = 7) SiO_2 compact. (b) Fracture surface of the same compact.

SUMMARY

Several important points are demonstrated by this research:

1. The controlled hydrolysis of alkoxides is a very powerful technique for controlling the bulk composition and dopant distribution in oxide powders. The technique is versatile and can be used to produce homogeneous or heterogeneous dopant distributions by paying careful attention to the synthetic procedures and the phase solubilities for the specific system. More importantly, controlled hydrolysis allows control over particle size and shape. Thus, "ideal" powders in the 0.1-1.0μm size range can be made as monodispersed spheroids of controlled chemical composition.

2. Careful attention to surface/liquid interfacial chemistry is a prerequisite for controlling the dispersion and packing of "ideal" powders into uniform, dense green microstructures. Green pieces with >68% of theoretical density are routinely obtained. SEM micrographs show that packing defects and/or voids are on the order of a particle diameter. Conversely, the improper dispersion and packing of the "ideal" powders results in green microstructures having a nonuniform and highly variable density; agglomerated regions and voids with a typical size of many (tens) particle diameters are typically observed.

3. Sintering experiments on uniformly packed compacts show that the monodispersed powders can be sintered at temperatures hundreds of degrees (400-500°C) lower than commercial powders, that the resulting microstructures have 98+% theoretical density, that the grains are small and are of the order of the initial particle size, and that no abnormal grain growth occurs.

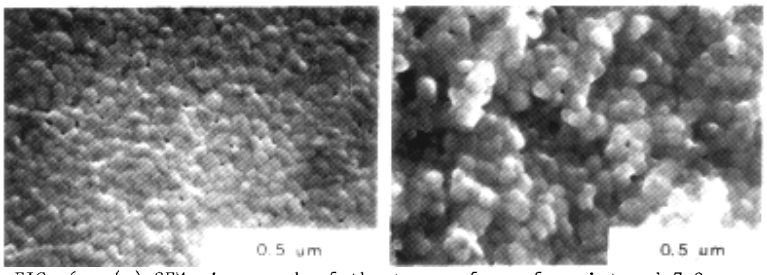

FIG. 6. (a) SEM micrograph of the top surface of a sintered ZrO_2 compact. Sintered for 1.5 hours at 1160°C. (b) SEM micrograph of the fracture surface of the same compact.

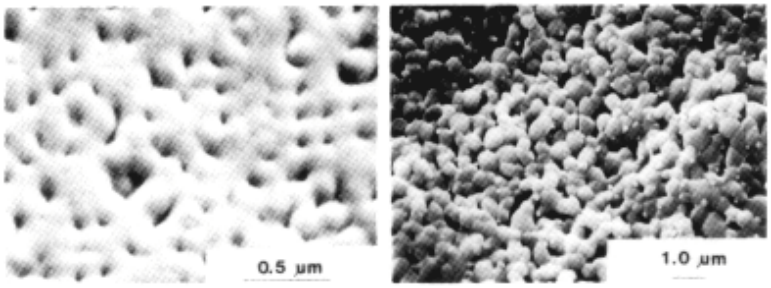

FIG. 7. (a) SEM micrograph of the top surface of a sintered (5 hours, 740°C) B-doped SiO_2 compact. (b) SEM micrograph of a sintered (2.5 hours, 1100°C) porous SrO-doped TiO_2 compact.

4. The use of monodispersed, spheroidal powders presents several practical advantages:
   a) Particle size and size distribution are easily determined by techniques such as light scattering.
   b) Monodispersed particles can be formed into ordered dispersions which can be studied by light diffraction techniques.
   c) Ability to test the sintering models developed over the past 3 decades by quantitatively studying sintering kinetics.
   d) Ability to control the sintered microstructure allows the careful study of microstructure-property relationships for electrical, magnetic, and mechanical properties.

ACKNOWLEDGMENTS

We acknowledge helpful discussions with H. K. Bowen and R. L. Pober. Also, we want to thank L. V. Janavicius, T. Kramer, D. Lange, P. Normile, L. Rigione, D. Todd, P. White, S. Woodhull, and W. Zamechek for analyses, photos, powder preparation, typing, and discussions.

REFERENCES

1. K. S. Mazdiyasni, Ceramics Intl. 8, 42 (1982).
2. E. A. Barringer and H. K. Bowen, Comm. Am. Ceram. Soc. 65, C199 (1982).
3. B. Fegley, H. K. Bowen, L. J. Rigione, and D. Todd, Bull. Am. Ceram. Soc. 62, 374 (1983).
4. W. Stober, A. Fink, and E. Bohn, J. Coll. Interf. Sci. 26, 62 (1968).
5. T. C. Huynh, A. Bleier, and H. K. Bowen, Bull. Am. Ceram. Soc. 61, 336 (1982).
6. B. Fegley, E. A. Barringer, and H. K. Bowen, Comm. Am. Ceram. Soc., in press (1984).
7. E. A. Barringer, N. Jubb, B. Fegley, R. L. Pober, and H. K. Bowen in: Int. Conf. on Ultra-Structure Processing of Ceramics, Classes and Composites, L. L. Hench and D. R. Ulrich, eds. (Wiley and Sons, NY 1984) pp. 000-000.
8. L. V. Janavicius, S.M. thesis, MIT (1984).
9. E. A. Barringer, B. Fegley, H. Okamura, P. Debeley, in preparation (1984).
10. R. L. Pober, R. Hay, M. L. Harris, in preparation (1984).
11. E. A. Barringer, Ph.D. thesis, MIT (1983).
12. B. Fegley, E. A. Barringer, D. Todd, in preparation (1984).
13. B. Fegley, P. White, H. Okamura, in preparation (1984).
14. H. C. Hamaker, Physica, 4, 1058 (1937).
15. B. Vincent, J. Coll. Interf. Sci., 42, 274 (1973).
16. J. Th. G. Overbeek, J. Coll. Interf. Sci., 58, 408 (1977).
17. R. H. Ottewill, J. Coll. Interf. Sci., 58, 357 (1977).
18. Th. F. Tadros in: The Effect of Polymers on Dispersion Properties, Th. F. Tadros, ed. (Academic Press, NY, 1982) pp. 1-38.
19. T. Sato and R. Ruch, "Stabilization of Colloidal Dispersions by Polymer Adsorption", (Marcel Dekker, NY, 1980), pp. 65-119.
20. M. V. Parish, R. R. Garcia, H. K. Bowen, in preparation (1984).
21. E. A. Barringer, B. E. Novich, and T. A. Ring, Accepted for publication in J. Coll. Interf. Sci.
22. W. H. Rhodes, J. Am. Ceram. Soc., 64, 19 (1981).
23. E. A. Barringer and H. K. Bowen in Int. Inst. for the Science of Sintering, 16, Belgrade, Yugoslavia, 1983.
24. E. A. Barringer, R. Brook, and H. K. Bowen in: Sixth Int. Conf. on Sintering and Related Phenomena Including Heterogeneous Catalysts, Notre Dame, 1983.
25. H. C. Ling and M. F. Yan, J. Mat. Sci., 18, 2688 (1983).

TABLE I. Chemical and Physical Properties of Monodispersed Oxide Powders

Material / Property	TiO_2 [2,11]	Singly-Doped TiO_2 [6]	Doubly-Doped TiO_2 [6]	ZrO_2 [12]	Doped ZrO_2 [13]	ZrO_2-Al_2O_3	SiO_2 [5]	Doped SiO_2 [8]
Chemical Precursor(s)	$Ti(OC_2H_5)_4$	$Ti(OC_2H_5)_4$	$Ti(OC_2H_5)_4$	$Zr(OC_3H_7)_4$ [c]	$Zr(OC_3H_7)_4$ [c]	$Zr(OC_3H_7)_4$ [c]	$Si(OC_2H_5)_4$	$Si(OC_2H_5)_4$
		$M(OC_2H_5)_5$ [a]	$M(OC_2H_5)_5$ [a]		$Y(OC_3H_7)_3$ [i]	sized Al_2O_3		$B(OC_4H_9)_3$
			$M'Cl_2$					
Dopant Level		0.1-1.0%(wt.)	0.1-1.0%(wt.)		6.5 mole %	<20 vol. %		<25%
Typical % Yield	70-80%	~70%	~70%	95% [d]	~45%	-	>95%	-
Average Size Range and Standard Deviation	-	-	-	-	-	- [f]	-	-
	d=0.3-0.7μm	d=0.3-0.7μm [e]	d=0.3-0.7μm [e]	d=0.2-0.3μm	d=0.2-0.3μm	d=0.25μm [f]	d-0.1-0.7μm	d=0.09-0.17μm
	σ_z =1.09	σ_z ~1.2 [e]	σ_z ~1.2 [e]	σ_z =1.2	σ_z =1.2	σ_z =1.22 [f]	σ_z =1.03	σ_z =1.04 [g]
Surface Area(m^2/g)	8-9 [h]			9-17 [h]				21 [h]
	170-200 [i]	200-250 [i]	100-300 [i]	28-57 [i]	66-72 [i]	34-65 [i]	30-40 [i]	
Shape	Spheroidal	Spheroidal	Spheroidal	Spheroidal	Spheroidal	Equiaxed	Spheroidal	Spheroidal
Structure	Unagglom-erated	Unagglom-erated	Unagglom-erated	Unagglom-erated	Unagglom-erated	Unagglom-rated	Unagglom-erated	Unagglom-erated
Crystal Form	Amorphous	Amorphous	Amorphous	Amorphous		Amorphous (ZrO_2)	Amorphous	Amorphous
Density (g/cm^3)	3.0-3.2	3.0-3.2	3.0-3.2	3.1	-	-	2.1	1.94
% Volatiles (H_2O+Carbon)	~12%	~20%	~20%	~20%	-	-	~8%	10-15%
Cation Impurities	Ca,Si	Ca,Si,Zr	Ca,Si,Zr	Al,Fe,Si,Hf	Al,Fe,Si, Hf	Ca,Fe,Si	-	Ca,Fe,Na

Notes and Abbreviations for Table I.

a) M = Nb, Ta b) M' = Ba, Cu, Sr c) n-propoxide and isopropoxide d) for Zr-isopropoxide

e) Visually estimated from SEM micrographs f) For sized Al_2O_3 powder before coating, see text.

g) B/Si = 1.0, 0.01 M TEOS concentration h) Alcohol washed powder i) Water washed powder